STUDY OF HOT METAL DESULFURIZATION EFFICIENCY THROUGH THE SOLID AND LIQUID PHASES FORMED IN THE MIXTURES*

Elton Volkers do Espírito Santo[1]
Silas Gambarine Soares[2]
Eduardo Junca[3]
Felipe Fardin Grillo[4]
José Roberto de Oliveira[5]

Abstract

The formation of solid phases around the CaO particle in hot metal desulfurization is reported in the literature as one of the main controller mechanisms on the process kinetics. Calcium sulfides, silicates and aluminates are the main compounds that hinder the sulfur diffusion to lime. Thus, the aim of this work is to elaborate desulfurizing mixtures that form different solid and liquid phases to develop a desulfurization efficiency predicting model, which was called Global Desulfurization Factor (FG_{DeS}). For this purpose, experimental desulfurization tests were carried out in a resistance furnace at a temperature of 1350°C, in an inert atmosphere with constant stirring of 500 rpm. Along with the tests, simulations were performed with FactSage 7.0 software in order to obtain the phases present in each mixture at the working temperature and compare them with the practical results. It was found that the tricalcium silicate phase (3CaO.SiO2) was present in the mixtures with the lowest desulfurization efficiency, which shows its kinetic limitation. In addition, the most efficient mixtures formed liquid phase above 20wt%, indicating that the CaO dissolved in the slag also participates in the desulfurization reaction.

Keywords: Desulfurization; Solid and Liquid Phases; Desulfurization Factor.

[1] *Metallurgical Engineer, Master's Degree Student, PROPEMM, Instituto Federal do Espírito Santo, Vitória, Espírito Santo, Brazil.*
[2] *MSc in Metallurgical and Materials Engeneering, Instituto Federal do Espírito Santo, Vitória, Espírito Santo, Brazil.*
[3] *PhD in Metallurgical and Materials Engeneering, Professor, PPGCEM, Universidade do Extremo Sul Catarinense, Criciúma, Santa Catarina, Brazil.*
[4] *PhD in Metallurgical and Materials Engeneering, Professor, Metallurgical and Materials Department, Instituto Federal do Espírito Santo, Vitória, Espírito Santo, Brazil*
[5] *PhD in Metallurgical Engeneering, Professor, PROPEMM, Instituto Federal do Espírito Santo, Vitória, Espírito Santo, Brazil*

** Technical contribution to the 51º Seminário de Fusão, Refino & Solidificação de Metais, part of the ABM Week 6th edition, June 7th-9th, 2022, São Paulo, SP, Brazil.*

1 INTRODUCTION

According to McFeaters and Fruehan [1], the formation of solid phases around the lime particles is related as one of the main controller mechanisms in the metal desulfurization. Those solid products (CaS, $2CaO.SiO_2$ e $3CaO.SiO_2$) control the kinetic process since it hinders the sulfur mass transfer into lime. Lindström and Sichen [2] also studied this solid phases precipitation and found, by EDS analysis, their presence around lime particle. Equation 1 shows the desulfurization reaction with silicon.

$$4CaO_{(s)} + 2\underline{S} + \underline{Si} = 2CaS_{(s)} + 2CaO.SiO_{2(s)} \quad \Delta G^0 = -488{,}680 + 161.26T\ (\frac{J}{mol}) \quad (1)$$

The aforementioned drawback may be minimized by a fluxing agent action, whose function is to dissolve these solid compounds into the liquid phase, decreasing the sulfur mass transfer resistance from the bath to the CaO surface. Fluorspar (CaF_2) has been used for this purpose due to its efficiency. According to Niedringhaus and Fruehan [3], it has a significant effect on the desulfurizing mixture up to 10wt%.
Grillo et al [4] determined that fluorspar is better fluxing than sodalite, since the synthetic slag using sodalite contained higher percentage of SiO_2. Other works used mixtures of CaO-Al system in the desulfurization process. Niedringhaus and Fruehan [3] results indicated that the optimum percentage of aluminum was between 0.15-0.30wt%. The authors reported the formation of a liquid film of calcium aluminate around the lime particle, which improved the desulfurization rate. On the other hand, the excess of aluminum formed solid phase of calcium aluminate, which decreased the desulfurization rate. Mitsuo et al [5] achieved similar results regarding aluminum pre-addition in desulfurizing mixtures. Equation 2 displays the desulfurization reaction using aluminum.

$$4CaO_{(s)} + 3\underline{S} + 2\underline{Al} = 3CaS_{(s)} + CaO.Al_2O_{3(S)} \quad \Delta G^0 = -898{,}964 + 291.5T\ (\frac{J}{mol}) \quad (2)$$

Classic models exist to determine the desulfurizing mixtures thermodynamic potential for removing sulfur from the bath. The following can be found: optical basicity (Λ), sulfide capacity (Cs) and sulfur partition (Ls). However, they have no relation to the desulfurization efficiency.
Therefore, it is important to know the parameters that influence the desulfurization kenetics (phases formed, percentage of solid and liquid phases and viscosity), since the limitation to obtain low sulfur contents is not thermodynamic, but kinetic.
According to Choi, Kim and Lee [6] the desulfurization rate is controlled by sulfur diffusion until the CaO particle (Equation 3).

$$-\frac{\mathrm{d}[\%S]}{\mathrm{dt}} = \mathrm{k}' \times \left(\frac{\mathrm{A}}{\mathrm{V_m}}\right) \times ([\%S]_t - [\%S]_{eq}) \quad (3)$$

Where A is the surface area between the CaO and the liquid metal (m^2); k is the global coefficient of mass transportation (m/min); V is the hot metal volume; $[\%S]_t$ is the sulfur percentage at time t; and $[\%S]_{eq}$ is the equilibrium sulfur percentage.
Thus, the solid phases formed around the CaO particles (CaS, $2CaO.SiO_2$, $3CaO.SiO_2$ and $CaO.Al_2O_3$) hamper the mass transport of the desulfurization process, which decreases both the efficiency and desulfurization rate. Therefore,

studies of desulfurizing mixtures and phases formation are fundamental to a better understanding of the desulfurization process.
Thermodynamic software are tools that allow the determination of these parameters and also helps to understand which type of mixture will be more efficient in industrial processes.
Hereupon, this work aim is to elaborate desulfurizing mixtures that form different solid and liquid phases. For this, materials such as calcitic lime, limestone fine, KR slag, fluorspar, sodalite, aluminum dross and boron oxide were used. The phases determination and percentage of solids and liquids in the mixtures at the temperature of the tests was performed using the FactSage 7.0 software. With these properties, a new parameter was developed to evaluate and predict the mixtures efficiency. This parameter was called “Desulfurization Factor”.

2 MATERIALS AND METHODS

2.1 Raw materials composition

The hot metal desulfurization tests were carried out using the following raw materials: calcitic lime, limestone fines, KR slag, fluorspar, standard flux, sodalite, boron oxide and aluminum dross. Their chemical composition is shown in Table 1. The initials for each raw material are next to its name.

Table 1. Raw materials chemical composition

Raw Material	Initials	Composition (wt%)													
		CaO	SiO_2	Al_2O_3	CaF_2	Fe_2O_3	MgO	K_2O	FeO	B_2O_3	MnO	Na_2O	S	C	P	Al
Calcitic Lime	C	98.84	0.67	0.05	0.00	0.08	0.21	0.00	0.00	0.00	0.00	0.00	0.08	0.0	0.06	0.00
Limestone Fine*	L	98.27	1.08	0.09	0.00	0.09	0.22	0.00	0.00	0.00	0.00	0.00	0.14	0.0	0.10	0.00
KR Slag	K	36.19	8.06	3.67	0.00	0.00	1.64	0.03	45.92	0.00	1.07	0.00	1.43	1.9	0.10	0.00
Fluorspar	F	3.87	12.04	5.79	72.12	4.34	0.00	1.83	0.00	0.00	0.00	0.00	0.00	0.0	0.00	0.00
Standard Flux	SF	3.80	26.80	22.37	0.00	0.00	1.74	3.06	0.00	0.00	0.32	26.37	0.03	0.0	0.00	15.51
Sodalite	S	0.00	51.95	22.73	0.00	3.79	1.08	6.39	0.00	0.00	0.00	14.07	0.00	0.0	0.00	0.00
Boron Oxide	B	0.00	0.00	0.00	0.00	0.00	0.00	0.00	0.00	100.0	0.00	0.00	0.00	0.0	0.00	0.00
Aluminum Dross	A	0.00	1.50	62.00	0.00	0.00	0.00	0.00	0.00	0.00	0.00	0.00	0.00	0.0	0.00	36.50

** After calcination*

The hot metal contained 94.6 wt% of Fe, 4.77 wt% of carbon, 0.042 wt% of sulfur, 0.29 wt% of silicon, 0.23 wt% of manganese and 0.060 wt% of phosphorus.

2.2 Desulfurizing mixtures

The proposed mixtures were defined in order to obtain different slag properties at the temperature of the experimental tests. Such properties are: present phases and percentage of solids and liquids. Table 2 displays the raw materials used in these mixtures, as well as their proportions.

Table 2. Mixtures and its raw materials proportion for the tests

Mixture	Quantity (wt%)							
	Calcitic Lime	Limestone Fine	KR Slag	Fluorspar	Standard Flux	Sodalite	Boron Oxide	Aluminum Dross
$C_{95}F_5$	95	-	-	5		-	-	-
$C_{88}SF_{12}$	88	-	-	-	12	-	-	-
$C_{74}L_8K_6SF_{12}$	74	8	6	-	12	-	-	-
$C_{81}L_8K_6B_5$	81	8	6	-	-	-	5	-
$C_{69}L_{15}K_6S_5F_5$	69	15	6	5	-	5	-	-
$C_{69}L_{15}K_6S_5B_5$	69	15	6	-	-	5	5	-
$C_{67}L_{15}K_6S_6A_6$	67	15	6	-	-	6	-	6
$C_{67}L_{15}K_6S_4A_4F_4$	67	15	6	4	-	4	-	4
$C_{67}L_{15}K_6S_4A_4B_4$	67	15	6	-	-	4	4	4

The mixtures nomenclature follows this logic: raw materials initials appear accompanied by their subscript percentage.

2.3 Determination of the phases present in the mixtures heating

The simulation of the equilibrium phases was carried out by FactSage 7.0 software. The equilibrium phases of the mixtures and slags used the FactPS, FToxid and FTMisc database. The Pure Solids sub-database in the FactPS database was used to determine the solid phases formed in the mixtures. The SlagH sub-database in the FToxid database was used to determine the liquid phases formed in the mixtures containing fluorspar. The SlagA sub-database was used in mixtures without fluorspar. The FTmisc database was applied to determine the equilibrium sulfur percentage using the Liquid sub-database. All simulation occurred at 1350°C and 1 atm. Table 3 displays the input data used in the thermodynamic programming.

Table 3. Chemical composition of the mixtures used as input data in the thermodynamic programming

Mixture	Composition (wt%)															Mass (g)
	CaO	SiO_2	Al_2O_3	CaF_2	Fe_2O_3	MgO	K_2O	FeO	B_2O_3	MnO	Na_2O	S	C	P	Al	
$C_{95}F_5$	15.35	0.20	0.05	0.59	0.05	0.03	0.01	0.00	0.00	0.00	0.00	0.01	0.00	0.01	0.00	16.31
$C_{88}SF_{12}$	14.21	0.62	0.44	0.00	0.01	0.06	0.06	0.00	0.00	0.01	0.51	0.01	0.00	0.01	0.30	16.25
$C_{74}L_8K_6SF_{12}$	14.21	0.73	0.50	0.00	0.01	0.08	0.06	0.47	0.00	0.02	0.54	0.03	0.02	0.01	0.32	16.99
$C_{81}L_8K_6B_5$	15.60	0.19	0.05	0.00	0.01	0.05	0.00	0.48	0.87	0.01	0.00	0.03	0.02	0.01	0.00	17.31
$C_{69}L_{15}K_6S_5F_5$	15.15	0.76	0.30	0.64	0.08	0.06	0.07	0.49	0.00	0.01	0.12	0.03	0.02	0.01	0.00	17.76
$C_{69}L_{15}K_6S_5B_5$	15.12	0.66	0.25	0.00	0.05	0.06	0.06	0.49	0.89	0.01	0.13	0.03	0.02	0.01	0.00	17.77
$C_{67}L_{15}K_6S_6A_6$	14.84	0.77	0.96	0.00	0.05	0.06	0.07	0.49	0.00	0.01	0.15	0.03	0.02	0.01	0.39	17.85
$C_{67}L_{15}K_6S_4A_4F_4$	14.83	0.66	0.69	0.51	0.07	0.06	0.06	0.49	0.00	0.01	0.10	0.03	0.02	0.01	0.26	17.80
$C_{67}L_{15}K_6S_4A_4B_4$	14.88	0.58	0.65	0.00	0.04	0.06	0.05	0.49	0.72	0.01	0.10	0.03	0.02	0.01	0.26	17.90

2.4 Desulfurization tests

To carry out the practical desulfurization tests an electric resistance furnace model MEV 1500/V, whose manufacturer is FORTELAB (Indústria de Fornos Elétricos LTDA), was used. An entrance was used to place an alumina tube for the argon injection in order to maintain the inert environment inside the furnace. Commercial argon was used at a flow rate of approximately 4 Nl/min and in none of the

experiments was noticed the slag formation before the desulfurizing agents addition which proves that the environment was inert.
Once the working temperature reached and stabilized, which was 1350 °C, the complete hot metal melting was verified through a secondary inlet. Then the desulfurizing materials were added and to aid in the additions a stainless steel tube was used to direct the material into the MgO-C crucible. The experimental apparatus and the stirrer type used are illustrated by Figure 1 (a) and (b).

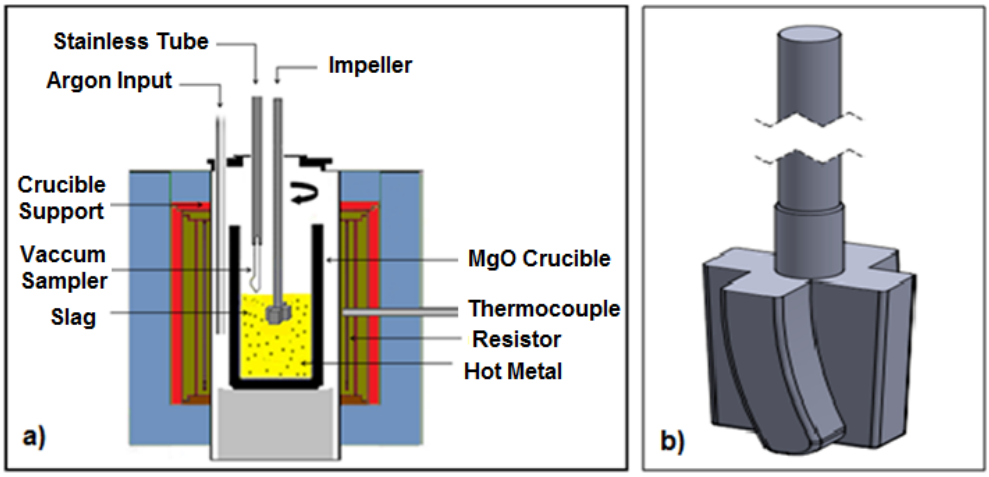

Figure 1. In a) schematic diagram of the experiments and in b) mechanical stirrer.

The reaction time was started immediately after mixture charging (time zero). Initial samples were taken at 3, 6, 9, 12, 15 and 25 minutes after the additions and each sample weighed approximately 10 grams. Sampling was also done through the entrance located in the furnace cover center using vacuum samplers.
The stirring was carried out by means of a mechanical stirrer with a constant rotation of 500 rpm which was positioned on the top of the furnace and its rod passed through the secondary entrance after the desulfurizing mixture addition. Stirring was interrupted with each sampling and then restarted and the stop time was always the same.

2.5 Desulfurization efficiency

The Desulfurization efficiency (Equation 4) was determined by the initial [%S_i] and final [%S_f] percentage of sulfur.

$$\eta(\%) = \frac{[\%S_i]-[\%S_f]}{[\%S_i]} \times 100 \quad (4)$$

3 RESULTS AND DISCUSSION

The experimental and thermodynamic results discussion was divided into the following steps: mixtures efficiency and Desulfurization Factor determination.

3.1 Mixtures efficiency

Table 4 shows the desulfurization mixtures efficiency after 25 minutes. Figure 2 displays the sulfur variation over time for those mixtures.

Table 4. Sulfur content variation over time and mixtures efficiencies

Mixture	%S variation over time (min)							Efficiency (25min)
	0	3	6	9	12	15	25	
$C_{69}L_{15}K_6S_5B_5$	0.0290	0.0200	0.0160	0.0092	0.0083	0.0069	0.0022	92.41
$C_{67}L_{15}K_6S_4A_4B_4$	0.0440	0.0390	0.0240	0.0220	0.0160	0.0110	0.0039	91.14
$C_{67}L_{15}K_6S_4A_4F_4$	0.0310	0.0260	0.0160	0.0120	0.0093	0.0075	0.0032	89.68
$C_{67}L_{15}K_6S_6A_6$	0.0270	0.0200	0.0160	0.0120	0.0092	0.0067	0.0036	86.67
$C_{95}F_5$	0.0570	0.0400	0.0340	0.0240	0.0220	0.0200	0.0110	80.70
$C_{69}L_{15}K_6S_5F_5$	0.0680	0.0560	0.0480	0.0470	0.0360	0.0250	0.0150	77.94
$C_{81}L_8K_6B_5$	0.0460	0.0390	0.0340	0.0280	0.0220	0.0210	0.0130	71.74
$C_{88}SF_{12}$	0.0330	0.0290	0.0250	0.0230	0.0200	0.0170	0.0100	69.70
$C_{74}L_8K_6SF_{12}$	0.0430	0.0320	0.0270	0.0240	0.0240	0.0220	0.0150	65.12

The representation ([%S]/[%Si]) is expressed as the relationship between sulfur content for each time and initial sulfur content. This was done due to the different initial sulfur contents in each test, so a comparison considering only the hot metal sulfur content at each time would be inconclusive. By making this relationship, all experiments start from the same point.

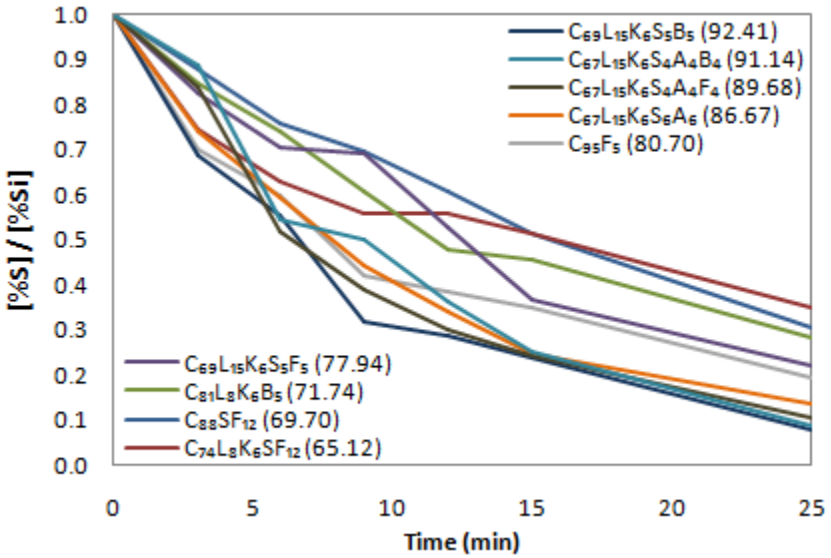

Figure 2. Sulfur variation ([%S]/[%Si]) over time.

It is observed that the $C_{69}L_{15}K_6S_5B_5$ mixture obtained the highest efficiency (92.41%). The three mixtures containing aluminum dross showed similar desulfurization performance, whose efficiencies lie between 86.67 and 91.14%. The $C_{95}F_5$ mixture is the last one with efficiency above 80%. It is noted that mixtures with many components showed, in general, better results. The combined addition of sodalite, aluminum dross and boron oxide or fluorspar indicates that these compounds have a fluxing effect on the slag, dissolving the solid compounds formed around the CaO particle and, consequently, promoting the sulfur mass transport in the system composed by metal, slag and solid lime. Note that the most efficient mixtures have 15wt% of limestone fine. The release of gases generated by carbonate calcination increases the system stirring, a fact that probably favored the desulphurization kinetics.

Table 5 shows the phases formed in mixtures heating.

Table 5. Phases formed in mixtures heating at 1350°C

Mixture	% Liq	% Sol	% Solid Phases					%Seq	Efficiency (%)
			CaO	CaS	MgO	$3CaO.SiO_2$	$3CaO.B_2O_3$		
$C_{69}L_{15}K_6S_5B_5$	31.45	68.56	67.71	0.29	0.00	0.00	0.00	2.17E-05	92.41
$C_{67}L_{15}K_6S_4A_4B_4$	33.87	66.13	60.49	0.00	0.00	5.64	0.00	2.14E-05	91.14
$C_{67}L_{15}K_6S_4A_4F_4$	28.78	71.22	70.88	0.34	0.00	0.00	0.00	2.15E-05	89.68
$C_{67}L_{15}K_6S_6A_6$	28.58	70.76	70.76	0.00	0.00	0.00	0.00	2.15E-05	86.67
$C_{95}F_5$	8.60	91.40	90.99	0.10	0.19	0.00	0.00	2.16E-05	80.79
$C_{69}L_{15}K_6S_5F_5$	23.61	76.39	75.69	0.36	0.13	0.00	0.00	2.22E-05	77.94
$C_{81}L_8K_6B_5$	11.94	88.06	76.24	0.36	0.00	0.00	9.48	2.21E-05	71.74
$C_{88}SF_{12}$	16.25	83.75	76.26	0.16	0.00	6.96	0.00	1.73E-05	69.70
$C_{74}L_8K_6SF_{12}$	17.02	82.98	69.94	0.36	0.00	11.09	0.00	2.08E-05	65.12

It is noted that the two mixtures with lower efficiencies were those with greater formation of tricalcium silicate ($3CaO.SiO_2$). McFeaters and Fruehan [1] indicate that this phase hinders the reaction kinetics by precipitating around the CaO particles and delaying sulfur diffusion. The equilibrium sulfur content cannot to be related to efficiency, which indicates that desulfurization depends mostly on factors that affect kinetics.

Despite the lower amounts of solid CaO produced in $C_{69}L_{15}K_6S_5B_5$ and $C_{67}L_{15}K_6S_4A_4B_4$ mixtures, they obtained the highest efficiencies. It is noted that in the first one there was only formation of CaS in small quantity (0.29wt%). On the other hand, the presence of 5.64wt% of $3CaO.SiO_2$ can be seen in the second. The formation of such a compound may not have had a negative effect on efficiency since the liquid phase fraction was high: the highest among all the mixtures. This may indicate that, for this situation, desulfurization also occurs inside the liquid phase, through the CaO dissolved in it, since its activity is equal to 1 (in all cases there is solid CaO formation, that is, the liquid is saturated with CaO). It is notorious that the four most efficient mixtures have a liquid phase formation above 25%. In this sense, there would be a reaction between two liquids, in whose interface the mass transport of sulfur would be favored.

3.2 Desulfurization Factor determination (F_{DeS})

Taking into account Equation 3, which shows that desulfurization is controlled by the mass transfer of sulfur to lime, and that CaS and $3CaO.SiO_2$ are the solid phases that can be formed in the mixtures used in this work, the expression of desulphurization factor becomes (Equation 5):

$$F_{DeS} = (\%CaO_S) - (\%3CaO.SiO_2 + \%CaS) \quad (5)$$

Desulfurization factor takes into account the mixtures chemical composition. Factors that affect kinetics cannot be different between the ones over which this analysis is carried out. The mixtures studied in this work are quite different regarding the materials used in their formulation. Therefore, for the desulphurization factor analysis, they were divided into groups so that the similar ones are analyzed together. In the present work, limestone fine and KR slag are materials that affect the desulphurization kinetics. The first one was used in different proportions (15wt%, 8wt% and 0wt%). As the decomposition of carbonates directly affects the process kinetics and this point cannot be measured thermodynamically by the phases

formation, the efficiency cannot be properly related to the desulfurization factor considering all mixtures in the same analysis. At the same time, the composition shown in Table 1 shows that the KR slag has 36wt% of CaO. The chemical analysis of the slag takes into account that the element exists in its most stable form, which in this case is CaO. As mentioned earlier, it is likely that an amount of CaO is already converted into CaS and 3CaO.SiO2, because it is the residue of the desulfurization process. Thus, CaO has already reacted and has the phases mentioned above formed around it. In addition, the remaining CaO probably has less reactivity than a virgin flux because it may already be sintered or hydrated. This affects the phases determination.
Therefore, the mixtures were grouped according to their limestone fine and KR slag quantities, keeping them always the same in which one. In this way, three groups were defined.

- **Group 1** – without limestone fine and KR slag: $C_{95}F_5$ and $C_{88}SF_{12}$;
- **Group 2** – 8wt% of limestone fine and 6wt% of KR slag: $C_{81}L_8K_6B_5$ and $C_{74}L_8K_6SF_{12}$;
- **Group 3** – 15wt% of limestone fine and 6wt% of KR slag: $C_{69}L_{15}K_6S_5F_5$, $C_{69}L_{15}K_6S_5B_5$, $C_{67}L_{15}K_6S_4A_4F_4$, $C_{67}L_{15}K_6S_4A_4B_4$ and $C_{67}L_{15}K_6S_6A_6$.

Equation 5 was used to determine the desulfurization factor for mixtures from groups 1 and 2. Table 10 shows their F_{DeS} and efficiency.

Table 6. Desulfurization factor and efficiency for mixtures from groups 1 and 2

Group	Mixture	F_{DeS}	η(%)
1	$C_{95}F_5$	90.89	80.70
1	$C_{88}SF_{12}$	69.14	69.70
2	$C_{81}L_8K_6B_5$	75.88	71.74
2	$C_{74}L_8K_6SF_{12}$	58.49	65.12

It can be noted that increasing the F_{DeS} also increases the desulphurization efficiency in both groups. Therefore, Equation 5 can be applied to evaluate the mixtures efficiency with characteristics of the groups 1 and 2.
Table 5 demonstrates that the mixtures from group 3 formed liquid phase between 23.61 to 33.87wt%. In addition, increasing the content of liquid slag decreases the percentage of solid CaO, since part of the CaO dissolves in the liquid and the desulfurization factor (Equation 5) also decreases. However, the desulfurization efficiency of the mixtures from group 3 (between 77.94 and 92.41%) was higher than the groups 1 and 2, which disagrees with the decreasing of the desulfurization factor.
The greater efficiency of the mixtures from group 3 may indicate that the CaO in the liquid part can desulfurize hot metal, once the CaO activity in the liquid fraction is 1. However, the desulfurization for mixtures containing up to 20wt% of liquid phases occurs predominantly by solid CaO.
Thus, Equation 6 demonstrates a new desulfurization factor, called Partial Desulfurization Factor (FP_{DeS}), proposed for mixtures with percentage of liquid phase higher than 20 wt%. FP_{DeS} considers the liquid CaO percentage ($\%CaO_L$).

$$FP_{DeS} = \%CaO_S + \%CaO_L - (\%3CaO.SiO_2 + \%CaS) \quad (6)$$

Figure 3 presents the graphs that relate the desulfurization factor (F_{DeS} and FP_{DeS}) with the efficiency for the group 3 mixtures.

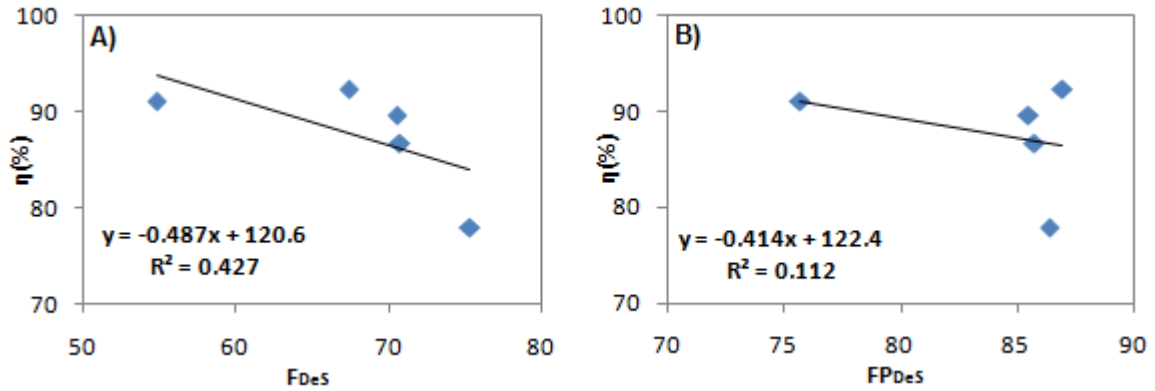

Figure 3. Relationship between the desulfurization factor versus desulfurization efficiency. A) F_{DeS}; B) FP_{DeS}.

Figure 3 shows a low coefficient of determination (R^2 = 0.427 and 0.112) between the desulfurization factor (F_{DeS} and FP_{DeS}) and desulfurization efficiency for mixtures from group 3. It is also observed a tendency in decreasing on the desulfurization efficiency with the increasing of the desulfurization factor. Such results indicate that the Equations 5 and 6 should not be used to determine the desulfurization factor of the mixtures from group 3.

This result prompted the search for a model that is representative for mixtures with such characteristics. Table 5 demonstrated that the mixtures from group 3 presented a content of liquid phase above of 20wt%. Thus, a new term was added to the FP_{DeS}. By multiplying the FP_{DeS} by the mass fraction of liquid (N_{Liq}) it was possible to obtain the desulfurization factor for mixtures with liquid formation above 20wt%, called Total Desulfurization Factor (FT_{DeS}). Equation 7 presents this new expression.

$$FT_{DeS} = [\%CaO_S + \%CaO_L - (\%3CaO.SiO_2 + \%CaS)] \times N_{Liq} \quad (7)$$

Table 7 displays the values of the three models for the mixtures from group 3, as well as the values of mass fraction of liquid (N_{Liq}) and liquid CaO content ($\%CaO_L$).

Table 7. Desulfurization factor (F_{DeS}, FP_{DeS} e FT_{DeS}) and desulfurization efficiency for mixtures from group 3

Mistura	$\%CaO_L$	N_{Liq}	F_{DeS}	FP_{DeS}	FT_{DeS}	η(%)
$C_{69}L_{15}K_6S_5B_5$	19.55	0.3145	67.42	86.97	27.35	92.41
$C_{67}L_{15}K_6S_4A_4B_4$	20.89	0.3387	54.85	75.74	25.65	91.14
$C_{67}L_{15}K_6S_4A_4F_4$	14.97	0.2878	70.54	85.51	24.61	89.68
$C_{67}L_{15}K_6S_6A_6$	15.00	0.2858	70.76	85.75	24.51	86.67
$C_{69}L_{15}K_6S_5F_5$	11.06	0.2361	75.33	86.39	20.40	77.94

Figure 5 shows the linear regression between FT_{DeS} and desulfurization efficiency.

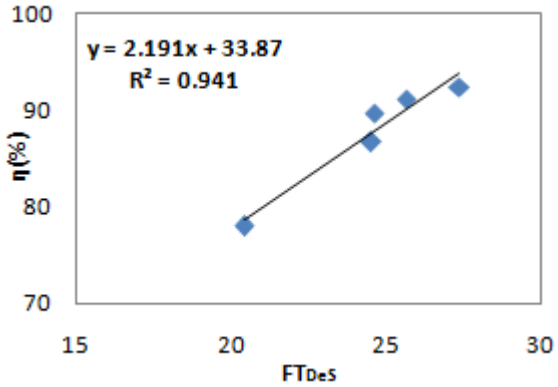

Figure 5. Linear regression between efficiency and FT_{DeS}.

Table 7 and Figure 5 show that increasing the FT_{DeS} also increases the desulfurization efficiency. Therefore, it can be affirmed that the higher the FT_{DeS} value more efficient is the mixture.
The coefficient of determination of 0.941 indicates that 94.10% of the efficiency variation can be explained by the variation of the FT_{DeS}. This shows that the linear regression model presented is satisfactory for predicting the desulfurization efficiency for this type of mixtures. Thus, efficiency can be obtained by the expression of Equation 8.

$$\eta(\%) = 2.191 \times (FT_{DeS}) + 33.87 \quad (8)$$

It is important to note that this model is applied only to mixtures with the same characteristics as those used in this work and under the same experimental conditions.
Although the mixtures from group 3 are more efficient than those from groups 1 and 2, their FT_{DeS} values are lower than the F_{DeS} values shown in Table 7, a fact that is not in agreement with the purpose of creating this parameter, that is: increasing the desulfurization factor also increases the mixture efficiency. Considering that a standardization of the desulfurization factor expression must be made, that is, that the mixture with the highest factor will always result in greater efficiency, a general model for mixtures with liquid phase formation above or below 20wt% is proposed. The Global Desulfurization Factor (FG_{DeS}) is presented by Equations 9 and 10.
Equation 9 is applied to mixtures with a liquid phase below 20wt%. It is observed that it is the same expression presented by Equation 5.

$$FG_{DeS} = (\%CaO_S) - (\%3CaO.SiO_2 + \%CaS) \quad (9)$$

Equation 10 is applied to mixtures with a liquid phase above 20wt%.

$$FG_{DeS} = [\%CaO_S + \%CaO_L - (\%3CaO.SiO_2 + \%CaS)] \times N_{Liq} \times k \quad (10)$$

k is the desulfurization constant, which adjusts the values of the desulfurization factor and was obtained empirically. For the mixtures studied in this work the value of k is equal to 4.24.
Thus, the higher the FG_{DeS} value the greater the desulfurization efficiency for all mixtures, as can be seen in Figure 6.

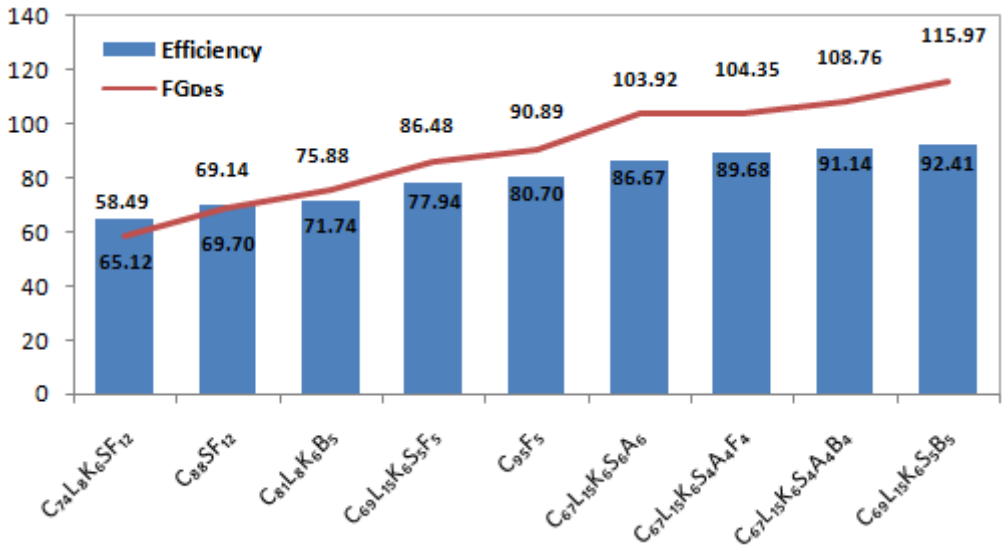

Figure 6. Values of desulfurization efficiency and FG_{Des} for the mixtures studied in this paper.

The FG_{Des} values present in the graph above correspond to those obtained by the models in Equations 9 and 10, which generalize the desulfurization factor for mixtures with a quantity of liquid below and above 20wt%.

4 CONCLUSION

The presence of a liquid phase above 20% resulted in greater desulfurization efficiency, while there was a decrease in it as the amount of solid phases increased (3CaO.SiO2 and CaS). In addition, the combined use of fluxing agents and limestone fine generated greater desulfurization efficiency.
The use of multicomponent mixtures with differences in kinetic factors prevents all of them from being analyzed together regarding the desulfurization factor. In relation to it, it was possible to obtain a linear regression model applicable to mixtures containing more than 20wt% of liquid phase, that is, those with 15wt% of limestone fine and 6wt% of KR slag.
The Global Desulfurization Factor (FG_{DeS}) for prediction of desulfurization efficiency was developed for mixtures with liquid phase below and above 20wt%, so that the highest factor always results in greater efficiency.

Acknowledgments

To CAPES, FAPES, CNPQ and PROPEMM for the technical and laboratory support.

REFERENCES

1 McFeaters LB, Fruehan RJ. Desulfurization of Bath Smelter Metal. Metallurgical Transactions B. 1993; 24: 441-447.
2 Lindström D, Sichen D. Kinetic Study on Desulfurization of Hot Metal Using CaO and CaC_2. Metallurgical and Materials Transactions B. 2015; 46: 83-92.
3 Niedringhaus JC, Fruehan RJ. Reaction Mechanism for the CaO-Al and CaO-CaF_2 Desulfurization of Carbon-Saturated Iron. Metallurgical Transactions B. 1988; 19: 261-268.
4 Grillo, FF, Sampaio RA, Viana JF, Espinosa DCR, Oliveira JR. Analysis of pig iron desulfurization with mixtures from the CaO-Fluorspar and CaO-Sodalite system with the

use of computational thermodynamics. REM: Revista Escola de Minas. 2013; 66: 461-465.

5 Mitsuo T, Shoji T, Hatta Y, Ono H, Mori H, Kai T. Improvement of Desulfurization by Addition of Aluminum to Hot Metal in the Lime Injection Process. Transactions of the Japan Institute of Metals. 1982; 23: 768-779.

6 Choi JY, Kim DJ, Lee HG. Reaction Kinetics of Desulfurization of Molten Pig Iron Using $CaO–SiO_2–Al_2O_3–Na_2O$ Slag Systems. ISIJ International. 2001; 41: 218-224.